iScience

CellPress

Article

Strains of *Staphylococcus aureus* that Colonize and Infect Skin Harbor Mutations in Metabolic Genes

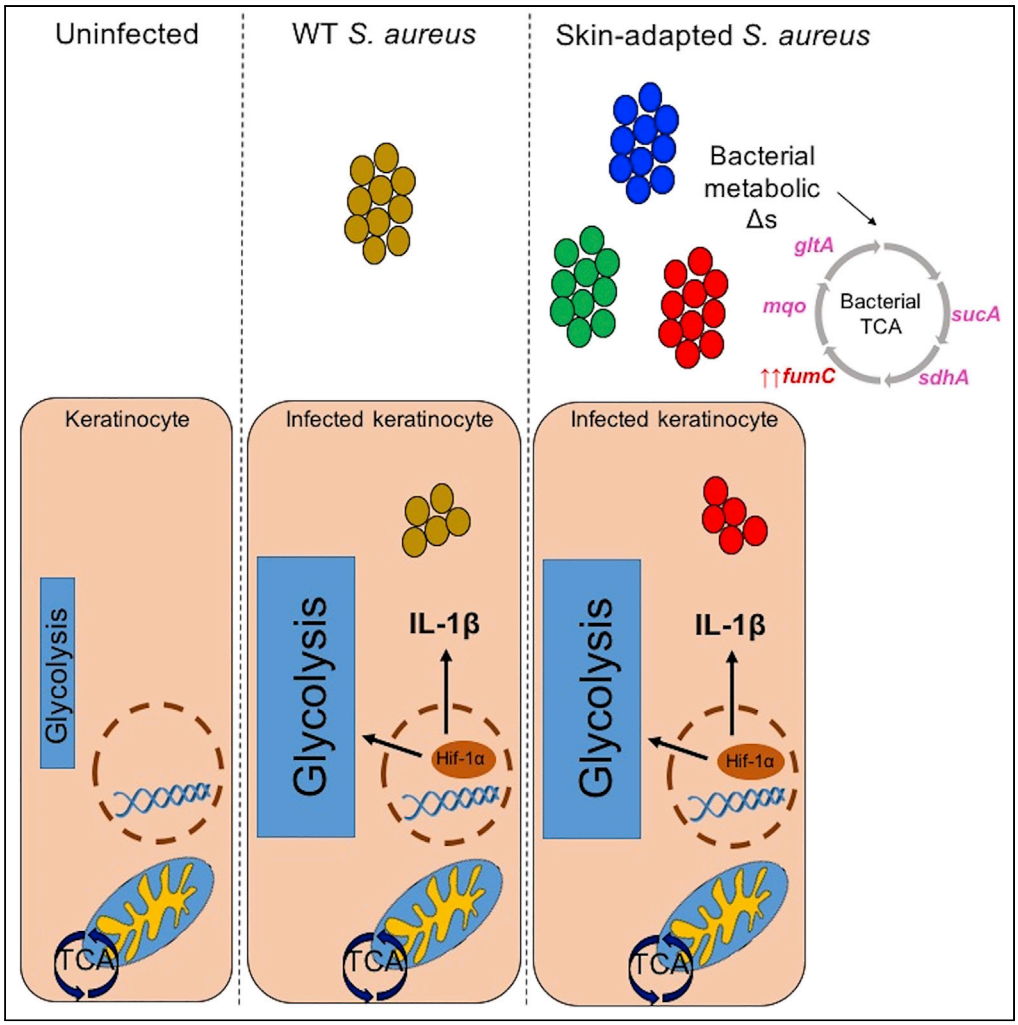

Karen P. Acker, Tania Wong Fok Lung, Emily West, ..., Christine Lauren, Paul J. Planet, Alice Prince

asp7@cumc.columbia.edu

HIGHLIGHTS

Staphylococcus aureus is a metabolically adaptive organism

Skin-adapted isolates harbor mutations in *fumC* and other metabolic genes

Novel metabolic gene variants were identified in skin-adapted strains

Acker et al., iScience *19*, 281–290
September 27, 2019
https://doi.org/10.1016/j.isci.2019.07.037

iScience

CellPress

Article

Strains of *Staphylococcus aureus* that Colonize and Infect Skin Harbor Mutations in Metabolic Genes

Karen P. Acker,[1,6,7] Tania Wong Fok Lung,[1,6] Emily West,[1,8] Joshua Craft,[1,9] Apurva Narechania,[4] Hannah Smith,[1] Kelsey O'Brien,[2] Ahmed M. Moustafa,[2] Christine Lauren,[3] Paul J. Planet,[1,2,4,5] and Alice Prince[1,10,*]

SUMMARY

***Staphylococcus aureus* is the most common cause of skin and soft tissue infections, yet the bacterial genetic changes associated with adaptation to human skin are not well characterized. *S. aureus* strains isolated from patients with chronic skin colonization and intermittent infection were used to determine the staphylococcal genotypes or phenotypes associated with adaptation to human skin. We demonstrate that polymorphisms in metabolic genes, particularly those involved in the tricarboxylic acid cycle, the fumarate-succinate axis, and the generation of terminal electron transporters, are unexpectedly common. These skin-adapted strains activated glycolysis and hypoxia-inducible factor-1α, interleukin (IL)-1β, and IL-18 release from keratinocytes and promoted dermatopathology equivalent to a methicillin-resistant *Staphylococcus aureus* USA300 control in a murine model of infection. However, in contrast to USA300, a skin-adapted isolate failed to generate protection from a secondary infectious challenge. Within the context of human skin, there appears to be selection for *S. aureus* metabolic adaptive changes that promote glycolysis and maintain pathogenicity.**

INTRODUCTION

Staphylococcus aureus is a ubiquitous organism that both colonizes human skin as an innocuous component of the commensal flora and causes invasive infection. The many surface proteins and toxins expressed by *S. aureus* that contribute to its ability to cause skin infection have been well characterized (Geoghegan et al., 2018), as has the inflammatory response that these proteins elicit. Less well understood is how *S. aureus* adapts to the human skin and maintains a state of chronic colonization and infection. To determine how *S. aureus* adapts to human skin, we studied a collection of isolates from children with atopic dermatitis (AD) who are colonized and repeatedly infected with *S. aureus* (Guzik et al., 2005; Park et al., 2013; Totte et al., 2016). Although many host factors have been found to contribute to *S. aureus* infection in AD (Kaesler et al., 2014; Krishna and Miller, 2012; Sehra et al., 2010), we were interested in determining the changes in the organisms that are associated with the ability to adapt to skin. Specific *S. aureus* clonal complexes, *agr* genotypes, and virulence factors have not been consistently linked to the pathogenesis of infection or colonization in AD (Benito et al., 2016; Fleury et al., 2017; Geoghegan et al., 2018; Yeung et al., 2011). The activation of a robust inflammatory response mediated by interleukin (IL)-1β is thought to be important in the clearance of *S. aureus* skin infection (Miller et al., 2007), but the contribution of specific proinflammatory toxins or surface proteins has not been linked to these infections.

The metabolic pathways used by *S. aureus* in the context of human skin are closely linked to inflammation. Immune cells as well as keratinocytes rapidly alter their metabolic activities upon bacterial stimulation using glycolysis to generate ATP and induce hypoxia-inducible factor (HIF) 1α, an important metabolic and proinflammatory transcription factor (Tannahill et al., 2013). *S. aureus* must use glycolysis and stimulate keratinocyte glycolysis to establish skin infection as demonstrated by the inability of Δ*pyk* mutants that are defective in glycolysis to infect skin (Vitko et al., 2015; Wickersham et al., 2017). Staphylococcal induction of keratinocyte glycolysis, even in the absence of toxin production, is sufficient to induce HIF1-α signaling and production of pro-IL-1β, a major proinflammatory cytokine (Wickersham et al., 2017). Activation of the inflammasome and IL-1β production in epithelial stem cells has been associated with epigenetic changes that confer protection from secondary challenge (Netea et al., 2016). This epigenetic reprogramming may be mediated by HIF-1α signaling (Cheng et al., 2014) and fumarate accumulation that modifies histone deacetylase activity and amplifies the cytokine response upon reinfection (Arts et al., 2016). Murine

[1]Department of Pediatrics, College of Physicians and Surgeons, Columbia University, New York, NY 10032, USA

[2]Children's Hospital of Philadelphia, Philadelphia, PA 19104, USA

[3]Department of Dermatology and Department of Pediatrics, College of Physicians and Surgeons, Columbia University, New York, NY 10032, USA

[4]Sackler Institute for Comparative Genomics, American Museum of Natural History, New York, NY, USA

[5]Department of Pediatrics, Perelman College of Medicine, University of Pennsylvania, Philadelphia, PA 19104, USA

[6]These authors contributed equally

[7]Present address: Department of Pediatrics, Weill Cornell Medicine, NY, NY 10021, USA

[8]Present address: Department of Dermatology, University of California at San Francisco, San Francisco, CA USA

[9]Present address: Department of Medicine, University of Maryland Medical Center, Baltimore, MD, USA

[10]Lead Contact

*Correspondence: asp7@cumc.columbia.edu

https://doi.org/10.1016/j.isci.2019.07.037

	Isolate #	EASI Score	Culture Site	Bacterial Burden	MRSA?	MLST(CC; *spa* Type)	Antibiotic Resistance
Low EASI	AD1	4.5	S	Few	MSSA	ST8(CC8; t1892)	EM
	AD2	0.2	S	Moderate	MSSA	ST1(CC1; t922)	
	AD3	2.4	P	Moderate	MRSA	ST22(CC22; new)	OX
	AD4	3.1	N	Few	MSSA	ST5 (CC5; t002)	EM
	AD5	2	S	Moderate	MSSA	ST15(CC15; new)	EM
High EASI	AD6	33.3	S	Heavy	MSSA	ST9 (CC109; t209)	EM
	AD7	33.6	S	Few	MSSA	ST? (CC188; t189)	
	AD8	40	S	Heavy	MSSA	ST5 (CC5; t045)	
	AD9	28.5	S	Few	MRSA	ST8 (CC8; t008)	CM, EM, LVX, OX, TC
	AD10	40	S	Heavy	MSSA	ST? (CC6; new)	EM

Table 1. Characteristics of *S. aureus* Strains Isolated from Patients with Atopic Dermatitis

CC, clonal complex; CM, clindamycin; EM, erythromycin; LVX, levofloxacin; MRSA, methicillin-resistant *Staphylococcus aureus*; N, nares; OX, oxacillin; P, perianal; S, skin; TC, tetracycline.

S. aureus isolates from low and high EASI (Eczema Area and Severity Index) score groups listed with site of culture, methicillin sensitivity, Ridom type, MLST, antibiotic resistance, and associated clinical EASI score.

Spa types labeled as "new" could not be assigned to a recognized type in the Ridom database, but had characteristics consistent with *spa* variable repeat regions.

skin infection with virulent *S. aureus* confers local protection from reinfection at the same site, due in part to increased macrophage populations in the skin that become primed and confer protective immunity to subsequent infection (Chan et al., 2017, 2018). We postulated that the organisms associated with infection and colonization in patients with AD are selected for their ability to evade local immune clearance mechanisms and that this selective process involves metabolic adaptation to the skin.

In the studies detailed in this report, we characterized a group of 10 *S. aureus* isolates associated with chronic colonization or infection from patients with AD. Although no consistent changes in the genes associated with pathogen-associated molecular pattern or toxin expression were found, there was a striking accumulation of genetic polymorphisms or variants and changes in expression of genes that affect the tricarboxylic acid (TCA) cycle enzymes and terminal electron acceptors, metabolic changes that were found to have important immunological consequences.

RESULTS

S. aureus Isolates Adapted to Human Skin Are Genotypically Diverse

From a collection of 134 *S. aureus* strains isolated from 79 patients, we selected 10 isolates from patients with the five highest and five lowest Eczema Area and Severity Index (EASI) scores as representing strains that had adapted to human skin. These skin-adapted strains (AD 1–10) were used for whole-genome sequencing, transcriptomic analysis, and phenotypic analysis (Table 1). Screening assays for selected virulence factors indicated substantial heterogeneity and a lack of correlation with clinical score. All the skin-adapted strains contained genes encoding many major toxins and adhesins, including *hla*, fibronectin-binding protein, and clumping factor (Figure 1A). The *hla* gene was present in all isolates, whereas in AD3, the gene contained a premature stop codon, which correlated with decreased Hla expression (Soong et al., 2015). AD3 and AD6 also lacked genes for the leukotoxin LukED. Genes for *arcA*-ACME, *speG*-ACME, *lukF*-PVL, and *lukS*-PVL were not present in any of these isolates, suggesting that none of the clinical isolates had the classical suite of accessory genes found in many USA300 strains. Whole-genome phylogenies were constructed using both SNP-based and amino acid-based approaches along with 30 previously sequenced, publically available isolates to contextualize genetic diversity (Figure 1B, Data S1 and S2). The results of the phylogenetic analysis, which agreed with clonal complex groupings as determined from multilocus sequence typing (MLST), showed a sporadic distribution mostly among CC8, CC1, and CC5, without clustering by clinical EASI score.

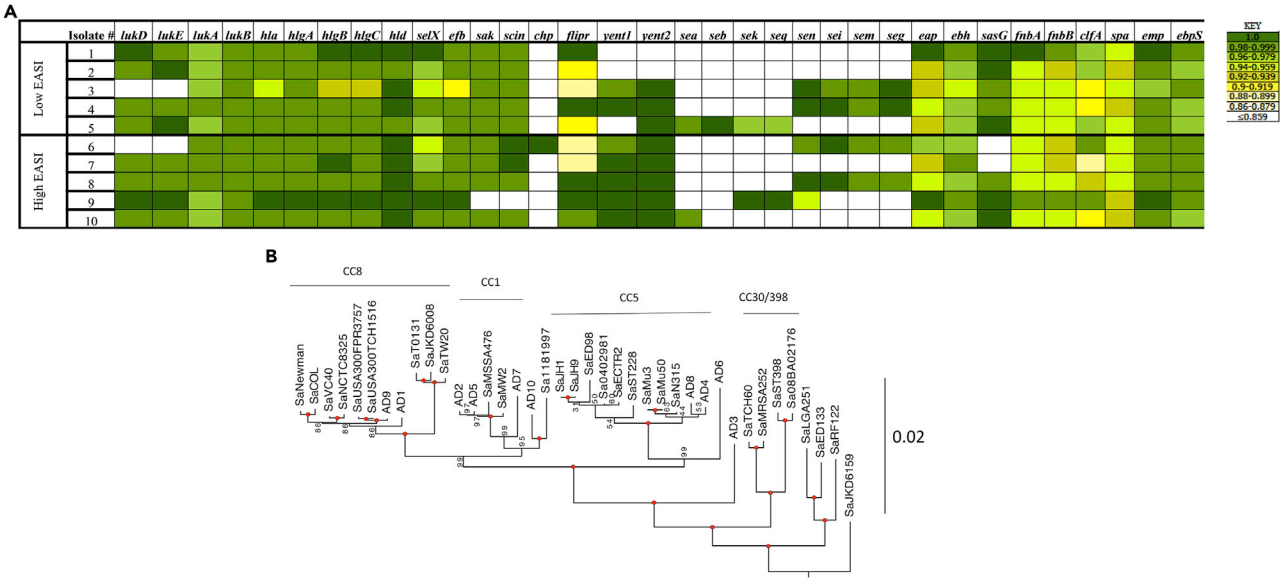

Figure 1. *S. aureus* Strains Isolated from Patients with Atopic Dermatitis Are Diverse

(A) Variable presence of toxin, resistance, and adhesion-associated genes. Heatmap display of Basic Local Alignment Search Tool (BLAST) results for specific gene sequence presence in each isolate compared with the reference strain USA300 FPR3757. Sequence identity (%) presented in KEY (right).

(B) Maximum likelihood phylogenetic tree from a concatenated open reading frame dataset, rooted with SaMSHR1132 (branch not shown). Bacterial isolates from patients with atopic dermatitis analyzed with 30 previously sequenced "sign-post" genomes that are publicly available. Values on or near the node are bootstrap support percentages; values of 100% are indicated with a red circle. The branch length reference is in substitutions/site.

See also Tables S1 and S2 and Data S1 and S2.

Skin-Adapted *S. aureus* Strains Have Variants in Metabolic Genes

Whole-genome sequence data were analyzed to determine if adaptation to skin was reflected in the selection of specific mutations or variants (Figures 2A–2D). When compared with the sequence of the well-studied reference genome USA300 FPR3757, each of the clinical isolates had numerous nonsynonymous SNPs for key components of the TCA cycle, the glycolytic pathway, or terminal components of the electron transport chain, sites of mutation typically present in staphylococcal small-colony variants (SCVs) (Proctor et al., 2006) (Figures 2A and 2B). As a way to establish the novelty of the SNPs that we identified, we used a Gene Novelty Unit (GNU) score to determine how many times a specific protein variant had been previously identified in all available annotated *S. aureus* genomes in the database (8,524 genomes available at NCBI) (Figures 2C and 2D). The proteins from each isolate were matched with the *S. aureus* database, and each protein given a score (GNU score) that is the number of exact matches in the entire database. We asked how abundant each of the variants in metabolic genes identified in our clinical strains was in the entire database and generated a heatmap based on the GNU score for each metabolic protein (Figure 2C). We observed that some were entirely novel (GNU score = 0), whereas others were found repeatedly in the isolates in the database (GNU score > 7,000). This analysis highlights several sequence variants that are completely new as well as proteins that have higher levels of novelty (lower GNU scores) overall, especially those in the terminal components of the electron transport chain and those involved in the succinate-fumarate axis. There was a striking number of nonsynonymous sequence polymorphisms and novel protein variants involved in bacterial handling of oxidant stress, namely, the SCV-associated menadione genes, *fumC,* and *fba* encoding aldolase in the glycolytic pathway, which is involved in the production of glyceraldehyde 3-phosphate (glyceraldehyde-3P). Glyceraldehyde-3P is a product of the pentose phosphate shunt, a substrate for glycolysis, and an important source of the anti-oxidant NADH. Note that the presence of SNPs or novel protein variants does not necessarily reflect loss of function, but may in fact be associated with increased or decreased expression and function of that locus. Although we did note many SNPs and novel protein variants in menadione, *hem*, and *mqo* loci, these were not associated with obvious growth defects. The lack of growth defects is not unexpected as these strains were recovered from the clinical microbiology laboratory, which was less likely to identify SCVs under their routine culture conditions given the ability of SCVs to rapidly revert to a wild-type (WT) phenotype (Becker et al., 2006; Tuchscherr et al., 2011). The SNPs and protein variants identified in known SCV

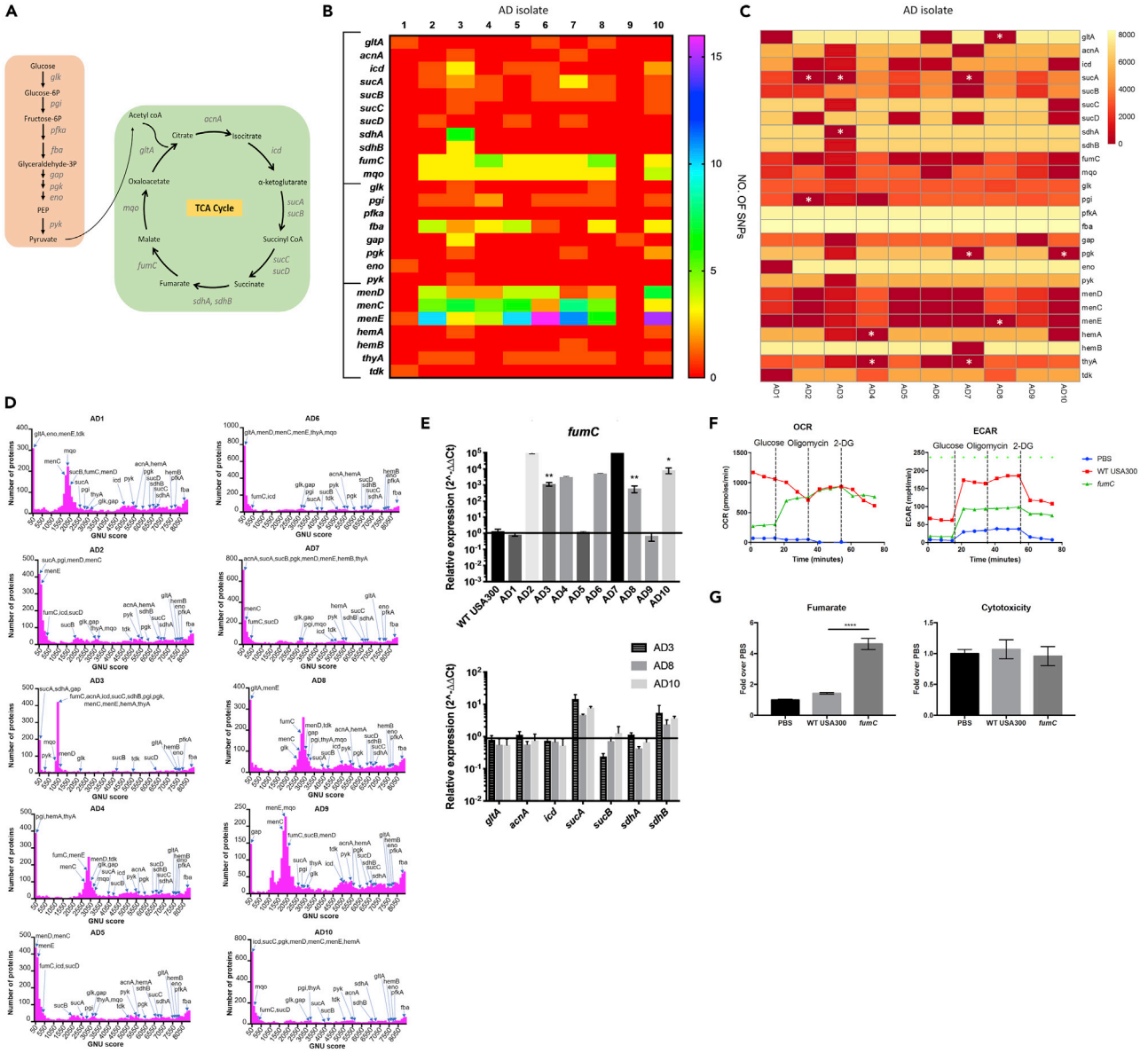

Figure 2. Skin-Adapted Isolates Harbor Metabolic Gene Variants

(A) Diagram of glycolysis and TCA cycle.

(B) Heatmap of number of nonsynonymous SNPs in skin-adapted isolates in TCA cycle, glycolytic, and SCV genes compared with the reference strain USA300 FPR3757.

(C) Heatmap of genes from 2B showing GNU score (number of exact protein matches [100% identity and 100% coverage]) in all known 8,524 *S. aureus* proteomes (as of 01/14/2019). Genes with 0 protein matches are indicated with a white asterisk.

(D) Ten histograms of GNU scores from 2C of all the proteins in each isolate. The x axis indicates the GNU score within a bin of 100 GNU scores in the *S. aureus* database, and the y axis indicates the number of proteins in the isolate's genome with a certain GNU score.

(E) qRT-PCR of TCA cycle genes in clinical *S. aureus* strains grown to exponential phase in lysogeny broth compared with USA300 WT LAC (representative graph of three individual experiments, n = 3 per condition). See also Table S3.

(F) Oxygen consumption rate (OCR) and extracellular acidification rate (ECAR) of uninfected HEKn cells and those stimulated with WT USA300 JE2 and *fumC* transposon mutant.

(G) Fumarate levels measured in cell media after 5-h infection in HEKn cells and associated cytotoxicity.

Each data point is the mean value ±SEM (n = 3) *p < 0.05, **p < 0.01, and ****p < 0.0001 by one-way (F) or two-way ANOVA (E).

genes were more heterogeneous in the database (Figure 2C), suggesting that these are not likely novel to our clinical isolates.

To put the GNU scores of these genes into the context of the entire genome and to get a sense of how many proteins in the genome have a similar number of exact hits, we plotted GNU score histograms with the y axis displaying the number of proteins in the genome that have matches in the databases within a bin of 100 GNU scores. Thus, for the 10 skin-adapted isolates that we analyzed, all had variants in metabolic genes that were very novel with GNU scores of <50 (Figure 2D). We interpret this finding as an indication that such novel variants are more abundant in our collection of *S. aureus* from the skin, when compared with all the isolates from diverse sites that are represented in the database.

Eight of 10 skin-adapted strains had SNPs in *fumC* compared with USA300 and all 10 isolates had lower GNU scores at this locus; 5 of 10 were variants seen in less than 500 strains in the database, and the other 5 were present in less than 3,000 of 8,524 annotated genomes available at NCBI (Figures 2B and 2C). FumC was of interest as we noted its dramatic upregulation in our clinical isolates (Figure 2E) along with *S. aureus* isolates associated with chronic pulmonary infection (Gabryszewski et al., 2019). Moreover, SNPs in genes involved in succinate metabolism (*sucA, B, C, D*), immediately upstream of fumarate in the TCA cycle, were present in 8/10 of the clinical strains from skin. Of these, 3 were completely novel protein variants in the SucA enzyme (Figure 2A) that converts α ketoglutarate into succinyl CoA, the succinate, and hence fumarate, precursor. The clinical isolate AD3 also had a completely novel protein sequence for SdhA, the enzyme that catalyzes the conversion of succinate to fumarate.

The variants that we identified could be associated with either increased or decreased gene expression. The *fumC* locus was upregulated in 7/10 isolates by 1,000–100,000 fold compared with USA300 (Figure 2E). Fumarate can suppress glycolysis by binding glyceraldehyde 3-phosphate dehydrogenase (GAPDH) (Kornberg et al., 2018), a key component of the glycolytic pathway generating pyruvate from glucose. Increased *fumC* expression would limit fumarate production and facilitate glycolysis, which is required for *S. aureus* proliferation in skin (Wickersham et al., 2017). This was confirmed by demonstrating that a *fumC* mutant was associated with less induction of glycolysis in keratinocytes *in vitro* (Figure 2F) and significantly greater accumulation of fumarate, but no apparent effects on cytotoxicity (Figure 2G). Thus, it appears that a major selective pressure for *S. aureus* adaptation to skin is metabolic as a result of its need to use glycolysis to generate ATP and may account for increased *fumC* expression in some strains as well as the numerous polymorphisms in other genes involved in the TCA cycle.

Genetic Changes Associated with Metabolic Adaptation Variably Impact Cytokine Induction

Given the metabolic genetic variants found in the skin isolates, we sought to determine the nature of the immune responses elicited in host keratinocytes and the association with glycolysis. We confirmed that three representative skin-adapted *S. aureus* strains and a USA300 control activate keratinocyte glycolysis (Figure 3A), a response attributed chiefly to keratinocyte metabolism (Figure 3B). The stabilization of HIF1α was stimulated by each of the *S. aureus* strains tested (Figure 3C). The IL-1 cytokines, IL-1β, IL-1α, IL-1RA, and IL-18, were each significantly suppressed in the absence of glycolysis (Figure 3D), an effect that was not due to cytotoxicity (Figure 3E) or differences in the uptake of the various strains by the keratinocytes (Figure 3F). The expression of the proinflammatory cytokines tumor necrosis factor (TNF)-α and IL-8, seemed to be compensatory, as their production was increased in keratinocytes treated with 2-deoxyglucose (2-DG). Induction of the monocyte or macrophage-specific cytokines and IL-17A was not dependent on glycolysis. Although we observed statistically significant differences in cytokine induction by the various strains, the biological relevance of these differences remains to be established.

Metabolic Adaptation Impairs Protection against Secondary Infection

A murine model of cutaneous infection was used to compare the pathogenicity of an AD isolate and the USA300 LAC control strain. We studied the responses to infection caused by strain AD3, which had increased *fumC* and *sucA* expression as well as a completely novel amino acid sequence in SucA. Having first established that AD3 and USA300 had similar *in vitro* growth rates (Figure S1), we showed that both strains caused similar amounts of dermonecrosis and were cleared equally well over 10 days of infection (Figures 4A and 4B). AD3 elicited a significantly greater amount of TNFα, IL-4, and IL-5 (Figure 4C), the latter two cytokines being consistent with the Th2-skewed response characteristic of previous studies of strains

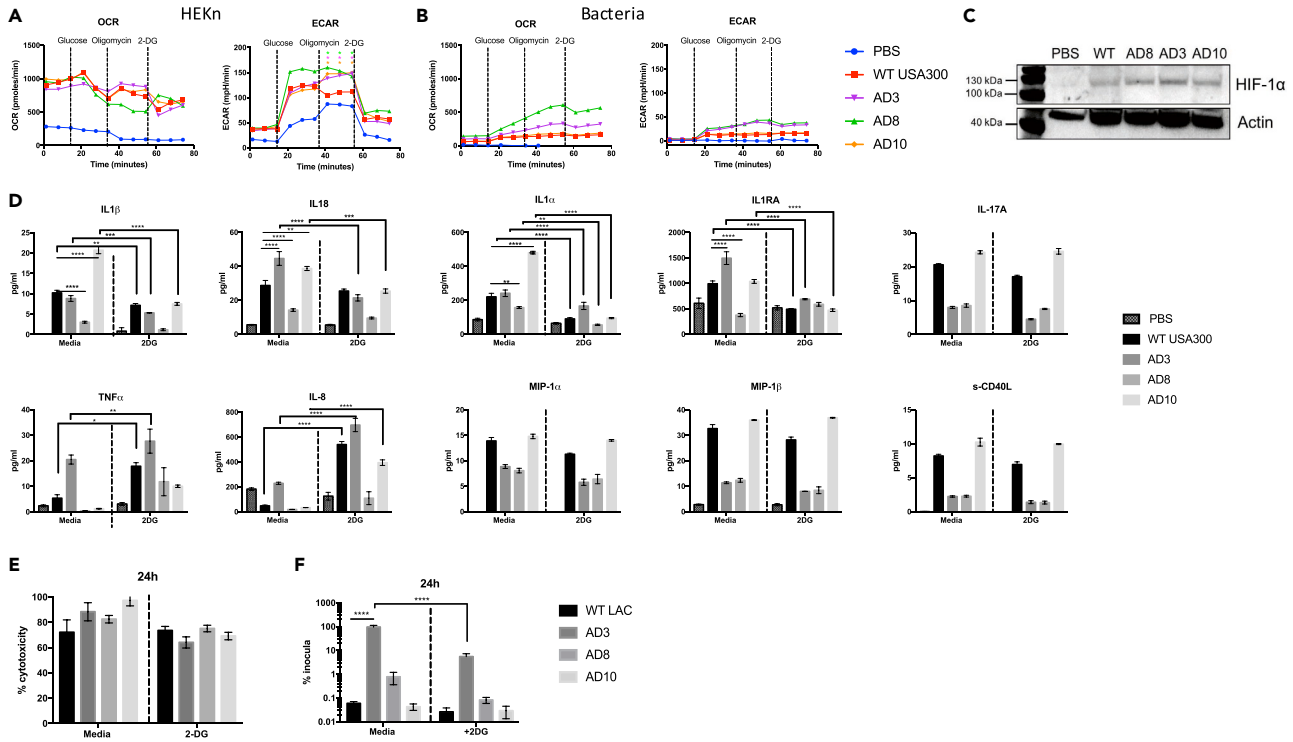

Figure 3. Skin-Adapted Strains Depend on Glycolysis to Stimulate Inflammatory Responses in Keratinocytes

(A and B) (A) OCR and ECAR of uninfected HEKns versus those stimulated with clinical AD strains and WT USA300 LAC *S. aureus* and (B) bacteria alone. Each data point is the mean value (n = 3) with *p < 0.05 by two-way ANOVA compared with WT.

(C) Immunoblots showing Hif1α in HEKn cells exposed to *S. aureus* for 4 h.

(D–F) (D) Cytokines measured by ELISA, and (E) cytoxicity and (F) intracellular persistence at 24 h in HEKn cells infected with *S. aureus* isolates and treated with and without 2-DG by lysostaphin protection assay. Each data point is the mean value ± SEM (n = 3 for cytotoxicity and cytokines, n = 9 for intracellular persistence), *p < 0.05, **p < 0.01, ***p < 0.001, and ****p < 0.0001 by two-way ANOVA.

from patients with AD (Mu et al., 2014). Immune cell recruitment into the skin lesions was also equivalent (Figure 4D).

As the impact of the metabolic changes in the skin-adapted strains was not manifested in acute immunogenicity, we postulated that the accrued polymorphisms in metabolic genes might impact the generation of local immune memory affecting the induction of protection to a repeated infectious challenge. We compared the ability of WT USA300 and AD3 to induce local protective immunity against a secondary infection. Following complete resolution of the initial infection, caused by either USA300 LAC or AD3, the animals were re-challenged at the same site with WT USA300. Mice primed with WT USA300 infection developed memory and had minimal lesions upon re-challenge, whereas those initially infected with AD3 had significantly larger areas of dermonecrosis upon USA300 re-challenge (Figures 4E and 4F). Thus the genetic differences in AD3 likely impact the generation of local protection to secondary *S. aureus* challenge, even though the initial response to infection appears similar to a non-adapted USA300 strain.

DISCUSSION

Based upon the genotypic and phenotypic characterization of *S. aureus* from chronically colonized patients, these studies illustrate that *S. aureus* dependence upon glycolysis for proliferation within the skin may promote the selection of strains with metabolic changes that promote glycolysis. We identified the accumulation of polymorphisms in genes likely to enhance glycolytic activity, limit the generation of fumarate, and in one case, prevent the development of local memory to secondary challenge. Our clinical strains were not phenotypically different from the isolates described in other reports characterizing strains from patients with AD (Byrd et al., 2017; Chiu et al., 2009; Kim et al., 2009), exhibiting substantial diversity and the presence of the genes encoding surface proteins and toxins typically associated with pathogenicity. However, genotypically, these isolates associated with chronic skin colonization or infection reflected a

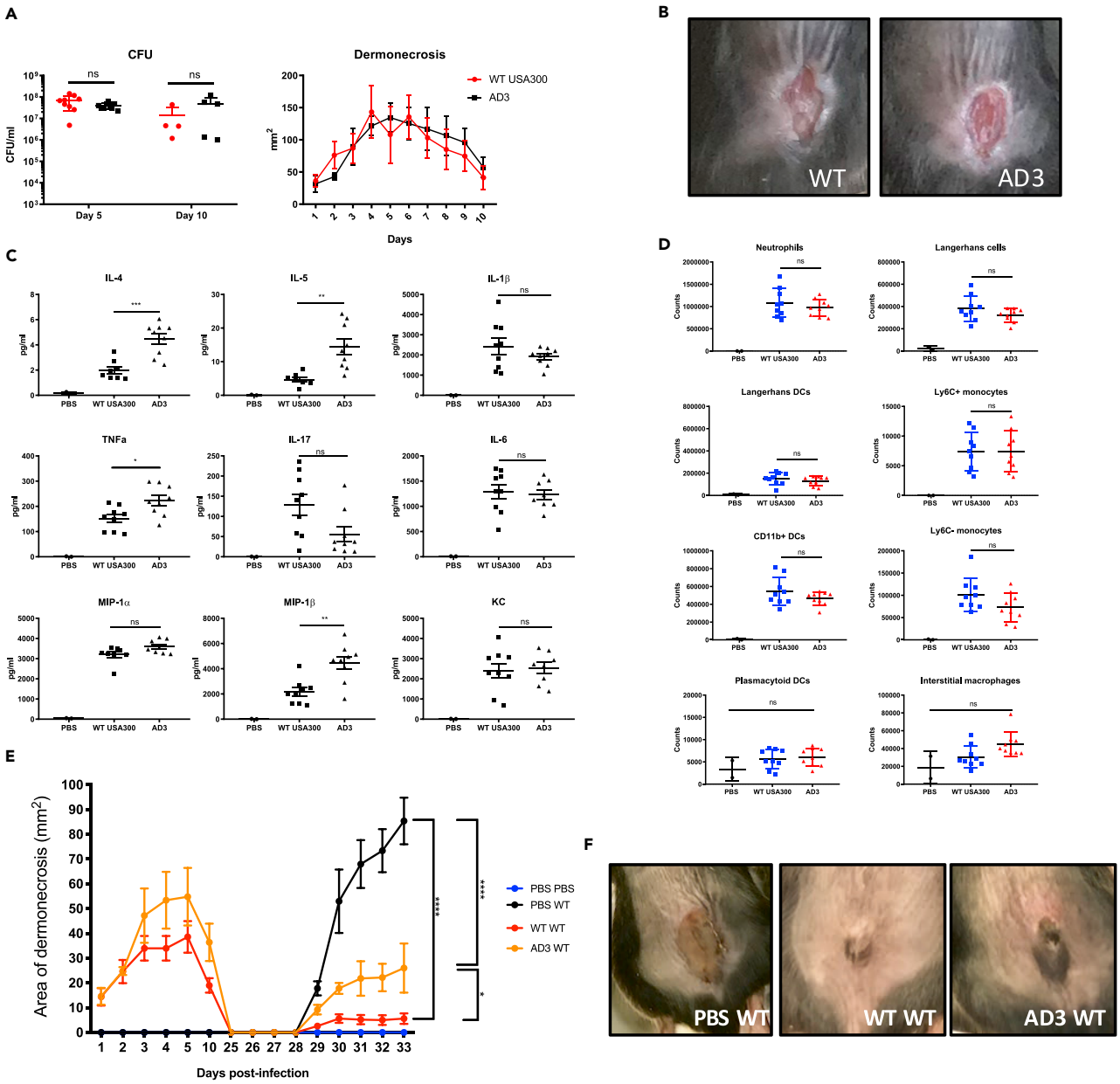

Figure 4. AD3 Generates Less Local Memory than USA300

(A) Bacterial load after 5 (n = 10) and 10 (n = 5) days, and dermonecrosis area over 10 days in mice intradermally infected with WT LAC or clinical isolate AD3.

(B) Images of mouse lesions after 5 days of infection.

(C) Cytokine measurements from skin biopsies of the infected sites after 5 days measured by ELISA.

(D) Immune cell recruitment 5 days after infection measured by fluorescence-activated cell sorting analysis. Results shown are pooled from two independent experiments.

(E) Area of dermonecrosis in mice infected with PBS, WT LAC, or AD3, followed by re-challenge at day 28 with WT LAC.

(F) Image of mouse lesions at day 33 from initial infection (5 days after challenge).

Each data point represents a mouse, and lines show mean values ± SEM. *p < 0.05, **p < 0.01, ***p < 0.001, ****p < 0.0001 determined by one- or two-way (E) ANOVA.

distinctive distribution of SNPs and protein variants in metabolic loci, many of which were not commonly found in the extensive collection of publically available *S. aureus* genomes. These multiple sequence variants in genes were associated with portions of the TCA cycle, as well as with loci involved in the production of terminal electron acceptors, including menadione and hemin loci, changes that are expected to

promote glycolysis. Our analysis of protein variants from clinical isolates associated with skin colonization or infection compared with the *S. aureus* isolates in the NCBI suggests that the majority of the organisms in the database, which are unlikely to be skin adapted, rarely contain this same collection of variants in genes involved in succinate and fumarate metabolism and suggests that these variants are selected within the context of skin infection.

The *fumC* locus was targeted in the skin-associated *S. aureus* strains, and several of these isolates had protein variants that were infrequent in the *S. aureus* genomic database. Some of these protein variants were identified in strains with over 100-fold induction of *fumC* expression along with differences in gene expression in additional loci that contribute to succinate-fumarate homeostasis. The presence of these metabolic variants suggests that regulation of fumarate is especially important for *S. aureus* to persist in the skin, which is consistent with the *S. aureus* requirement for glycolysis to support its bioenergetic activity in the skin (Vitko et al., 2015; Wickersham et al., 2017). There are several possible roles for fumarate and *fumC* in *S. aureus* metabolism. The expression of *fumC* may be upregulated for fumarate utilization as a carbon source when glucose is limited (Michalik et al., 2017; Surmann et al., 2014), or fumarate may function to decrease oxidant stress, as it increases glutathione, a major oxidant trap within the cell. Another possibility is that the SNPs identified in our isolates may result in FumC inactivation leading to upregulation of *fumC* expression by the host cell to compensate for fumarate accumulation within the cell. Most consistent with our findings is fumarate suppression of aerobic glycolysis by binding directly to GAPDH, which provides substrates for glycolytic metabolism (Kornberg et al., 2018). Hence, increased *fumC* expression by *S. aureus* isolates may lead to increased fumarate hydrolysis and prevent suppression of glycolysis. Of note, fumarate is also associated with selective effects on CD4 versus CD8 T cell function and the induction of IL-4 production (Ghoreschi et al., 2011; Mills et al., 2018), an immunological phenotype characteristic of AD (Weidinger et al., 2018).

The reliance of *S. aureus* upon glycolysis for its bioenergetic needs in the setting of keratinocyte infection provides a unifying theme to help explain the diversity in the phenotypes and genotypes of strains associated with skin infection in humans. As previously established, staphylococcal induction of glycolysis is associated with the stabilization of HIF-1α and IL-1β production (Wickersham et al., 2017). Although not all the proinflammatory genes activated in keratinocytes by *S. aureus* were influenced by glycolysis, the major members of the IL-1 family including IL-1β, an important factor in an effective response to skin infection (Miller et al., 2007), were suppressed in the presence of 2-DG. Despite variability in the presence of toxin and other virulence genes, the inherent immunostimulatory response to *S. aureus* induction of glycolysis was sufficient to activate a robust immune response. This helps to explain how even *agr* mutants and strains lacking toxins could be associated with AD flares (Soong et al., 2015).

A major goal of this study was to establish the genetic changes in *S. aureus* that facilitate chronic skin infection. We demonstrate that there are metabolic changes in skin-adapted strains that function to promote staphylococcal glycolytic activity. We compared two unrelated strains with distinct phenotypes, a skin-adapted AD strain and a virulent USA300 LAC, which both activated similar immune responses and dermonecrosis, but had very different metabolic profiles. Although *S. aureus* is highly adapted to evade host immune responses, our studies indicate that adaptation to the local metabolic milieu is also important in the skin. Numerous epithelial and immune defects may contribute to the susceptibility of patients with AD to *S. aureus* infection. Our data indicate that the ability of *S. aureus* to adapt to the metabolic conditions imposed by skin is critical in establishing *S. aureus* colonization as well as susceptibility to reinfection.

Limitations of the Study

Comparing clinical strains genotypically is limited by the difficulty in establishing an appropriate reference strain for each clinical isolate, and thus the variability in the genotypic background cannot be entirely accounted for, which is why we developed a GNU score to better appreciate the significance of the SNPs identified in these strains. The phenotypic analysis of local immune memory was limited by using two strains with varying genetic backgrounds, and thus we can postulate but cannot deduce that the differing response is due to metabolic differences between a skin-adapted and WT strain.

METHODS

All methods can be found in the accompanying Transparent Methods supplemental file.

SUPPLEMENTAL INFORMATION

Supplemental Information can be found online at https://doi.org/10.1016/j.isci.2019.07.037.

ACKNOWLEDGMENTS

This work was supported by NIH grant R01AI103854 to A.P., NIH grants 1K08AI101005 and 1R01AI137526-01 to P.J.P., NIH grant S10RR027050 to the Columbia Center for Translational Immunology Flow Cytometry Core, and NIH NIAID T32 Training Grant in Pediatric Infectious Diseases (AI007531).

AUTHOR CONTRIBUTIONS

Conceptualization, K.P.A., T.W.F.L., A.P., P.J.P., C.L., and E.W.; Formal Analysis and Investigation, K.P.A., T.W.F.L, E.W., J.C., A.N., H.S., K.O., A.M.M., C.L., and P.J.P.; Writing – Original Draft, K.P.A. and A.P.; Writing – Review and Editing: K.P.A., T.W.F.L., A.P., P.J.P., and A.M.M.; Funding Acquisition, A.P. and P.J.P.; Supervision: P.J.P. and A.P.

DECLARATION OF INTERESTS

The authors declare no competing interests.

Received: February 13, 2019
Revised: July 22, 2019
Accepted: July 23, 2019
Published: September 27, 2019

REFERENCES

Arts, R.J., Novakovic, B., Ter Horst, R., Carvalho, A., Bekkering, S., Lachmandas, E., Rodrigues, F., Silvestre, R., Cheng, S.C., Wang, S.Y., et al. (2016). Glutaminolysis and fumarate accumulation integrate immunometabolic and epigenetic programs in trained immunity. Cell Metab. *24*, 807–819.

Becker, K., Laham, N.A., Fegeler, W., Proctor, R.A., Peters, G., and von Eiff, C. (2006). Fourier-transform infrared spectroscopic analysis is a powerful tool for studying the dynamic changes in Staphylococcus aureus small-colony variants. J. Clin. Microbiol. *44*, 3274–3278.

Benito, D., Aspiroz, C., Gilaberte, Y., Sanmartin, R., Hernandez-Martin, A., Alonso, M., Gomez, P., Lozano, C., and Torres, C. (2016). Genetic lineages and antimicrobial resistance genotypes in Staphylococcus aureus from children with atopic dermatitis: detection of clonal complexes CC1, CC97 and CC398. J. Chemother. *28*, 359–366.

Byrd, A.L., Deming, C., Cassidy, S.K.B., Harrison, O.J., Ng, W.I., Conlan, S., Belkaid, Y., Segre, J.A., and Kong, H.H. (2017). Staphylococcus aureus and Staphylococcus epidermidis strain diversity underlying pediatric atopic dermatitis. Sci. Transl. Med. *9*, eaal4651.

Chan, L.C., Chaili, S., Filler, S.G., Miller, L.S., Solis, N.V., Wang, H., Johnson, C.W., Lee, H.K., Diaz, L.F., and Yeaman, M.R. (2017). Innate immune memory contributes to host defense against recurrent skin and skin structure infections caused by methicillin-resistant Staphylococcus aureus. Infect. Immun. *85*, e00876–16.

Chan, L.C., Rossetti, M., Miller, L.S., Filler, S.G., Johnson, C.W., Lee, H.K., Wang, H., Gjertson, D., Fowler, V.G., Jr., Reed, E.F., et al. (2018). Protective immunity in recurrent Staphylococcus aureus infection reflects localized immune signatures and macrophage-conferred memory. Proc. Natl. Acad. Sci. U S A *115*, E11111–E11119.

Cheng, S.C., Quintin, J., Cramer, R.A., Shepardson, K.M., Saeed, S., Kumar, V., Giamarellos-Bourboulis, E.J., Martens, J.H., Rao, N.A., Aghajanirefah, A., et al. (2014). mTOR- and HIF-1alpha-mediated aerobic glycolysis as metabolic basis for trained immunity. Science *345*, 1250684.

Chiu, L.S., Ho, M.S., Hsu, L.Y., and Tang, M.B. (2009). Prevalence and molecular characteristics of Staphylococcus aureus isolates colonizing patients with atopic dermatitis and their close contacts in Singapore. Br. J. Dermatol. *160*, 965–971.

Fleury, O.M., McAleer, M.A., Feuillie, C., Formosa-Dague, C., Sansevere, E., Bennett, D.E., Towell, A.M., McLean, W.H.I., Kezic, S., Robinson, D.A., et al. (2017). Clumping factor B promotes adherence of staphylococcus aureus to corneocytes in atopic dermatitis. Infect. Immun. *85*, e00994–16.

Gabryszewski, S.J., Wong Fok Lung, T., Annavajhala, M.K., Tomlinson, K.L., Riquelme, S.A., Khan, I.N., Noguera, L.P., Wickersham, M., Zhao, A., Mulenos, A.M., et al. (2019). Metabolic adaptation in MRSA pneumonia. Am. J. Respir. Cell Mol. Biol. *61*, 185–197.

Geoghegan, J.A., Irvine, A.D., and Foster, T.J. (2018). Staphylococcus aureus and atopic dermatitis: a complex and evolving relationship. Trends Microbiol. *26*, 484–497.

Ghoreschi, K., Brück, J., Kellerer, C., Deng, C., Peng, H., Rothfuss, O., Hussain, R.Z., Gocke, A.R., Respa, A., Glocova, I., et al. (2011). Fumarates improve psoriasis and multiple sclerosis by inducing type II dendritic cells. J. Exp. Med. *208*, 2291–2303.

Guzik, T.J., Bzowska, M., Kasprowicz, A., Czerniawska-Mysik, G., Wojcik, K., Szmyd, D., Adamek-Guzik, T., and Pryjma, J. (2005). Persistent skin colonization with Staphylococcus aureus in atopic dermatitis: relationship to clinical and immunological parameters. Clinical and experimental allergy. J. Br. Soc. Allergy Clin. Immunol. *35*, 448–455.

Kaesler, S., Volz, T., Skabytska, Y., Koberle, M., Hein, U., Chen, K.M., Guenova, E., Wolbing, F., Rocken, M., and Biedermann, T. (2014). Toll-like receptor 2 ligands promote chronic atopic dermatitis through IL-4-mediated suppression of IL-10. J. Allergy Clin. Immunol. *134*, 92–99.

Kim, D.W., Park, J.Y., Park, K.D., Kim, T.H., Lee, W.J., Lee, S.J., and Kim, J. (2009). Are there predominant strains and toxins of Staphylococcus aureus in atopic dermatitis patients? Genotypic characterization and toxin determination of S. aureus isolated in adolescent and adult patients with atopic dermatitis. J. Dermatol. *36*, 75–81.

Kornberg, M.D., Bhargava, P., Kim, P.M., Putluri, V., Snowman, A.M., Putluri, N., Calabresi, P.A., and Snyder, S.H. (2018). Dimethyl fumarate targets GAPDH and aerobic glycolysis to modulate immunity. Science *360*, 449–453.

Krishna, S., and Miller, L.S. (2012). Innate and adaptive immune responses against Staphylococcus aureus skin infections. Semin. Immunopathol. *34*, 261–280.

Michalik, S., Depke, M., Murr, A., Gesell Salazar, M., Kusebauch, U., Sun, Z., Meyer, T.C., Surmann, K., Pförtner, H., Hildebrandt, P., et al. (2017). A global Staphylococcus aureus proteome resource applied to the in vivo characterization of host-pathogen interactions. Sci. Rep. *7*, 9718.

Miller, L.S., Pietras, E.M., Uricchio, L.H., Hirano, K., Rao, S., Lin, H., O'Connell, R.M., Iwakura, Y., Cheung, A.L., Cheng, G., et al. (2007). Inflammasome-mediated production of IL-1beta is required for neutrophil recruitment against Staphylococcus aureus in vivo. J. Immunol. *179*, 6933–6942.

Mills, E.A., Ogrodnik, M.A., Plave, A., and Mao-Draayer, Y. (2018). Emerging understanding of the mechanism of action for dimethyl fumarate in the treatment of multiple sclerosis. Front. Neurol. *9*, 5.

Mu, Z., Zhao, Y., Liu, X., Chang, C., and Zhang, J. (2014). Molecular biology of atopic dermatitis. Clin. Rev. Allergy Immunol. *47*, 193–218.

Netea, M.G., Joosten, L.A., Latz, E., Mills, K.H., Natoli, G., Stunnenberg, H.G., O'Neill, L.A., and Xavier, R.J. (2016). Trained immunity: a program of innate immune memory in health and disease. Science *352*, aaf1098.

Park, H.Y., Kim, C.R., Huh, I.S., Jung, M.Y., Seo, E.Y., Park, J.H., Lee, D.Y., and Yang, J.M. (2013). Staphylococcus aureus colonization in acute and chronic skin lesions of patients with atopic dermatitis. Ann. Dermatol. *25*, 410–416.

Proctor, R.A., von Eiff, C., Kahl, B.C., Becker, K., McNamara, P., Herrmann, M., and Peters, G. (2006). Small colony variants: a pathogenic form of bacteria that facilitates persistent and recurrent infections. Nat. Rev. Microbiol. *4*, 295–305.

Sehra, S., Yao, Y., Howell, M.D., Nguyen, E.T., Kansas, G.S., Leung, D.Y., Travers, J.B., and Kaplan, M.H. (2010). IL-4 regulates skin homeostasis and the predisposition toward allergic skin inflammation. J. Immunol. *184*, 3186–3190.

Soong, G., Paulino, F., Wachtel, S., Parker, D., Wickersham, M., Zhang, D., Brown, A., Lauren, C., Dowd, M., West, E., et al. (2015). Methicillin-resistant Staphylococcus aureus adaptation to human keratinocytes. mBio *6*, e00289–15.

Surmann, K., Michalik, S., Hildebrandt, P., Gierok, P., Depke, M., Brinkmann, L., Bernhardt, J., Salazar, M.G., Sun, Z., Shteynberg, D., et al. (2014). Comparative proteome analysis reveals conserved and specific adaptation patterns of Staphylococcus aureus after internalization by different types of human non-professional phagocytic host cells. Front. Microbiol. *5*, 392.

Tannahill, G.M., Curtis, A.M., Adamik, J., Palsson-McDermott, E.M., McGettrick, A.F., Goel, G., Frezza, C., Bernard, N.J., Kelly, B., Foley, N.H., et al. (2013). Succinate is an inflammatory signal that induces IL-1beta through HIF-1alpha. Nature *496*, 238–242.

Totte, J.E., van der Feltz, W.T., Hennekam, M., van Belkum, A., van Zuuren, E.J., and Pasmans, S.G. (2016). Prevalence and odds of Staphylococcus aureus carriage in atopic dermatitis: a systematic review and meta-analysis. Br. J. Dermatol. *175*, 687–695.

Tuchscherr, L., Medina, E., Hussain, M., Volker, W., Heitmann, V., Niemann, S., Holzinger, D., Roth, J., Proctor, R.A., Becker, K., et al. (2011). Staphylococcus aureus phenotype switching: an effective bacterial strategy to escape host immune response and establish a chronic infection. EMBO Mol. Med. *3*, 129–141.

Vitko, N.P., Spahich, N.A., and Richardson, A.R. (2015). Glycolytic dependency of high-level nitric oxide resistance and virulence in Staphylococcus aureus. mBio *6*, e00045–15.

Weidinger, S., Beck, L.A., Bieber, T., Kabashima, K., and Irvine, A.D. (2018). Atopic dermatitis. Nat. Rev. Dis. Primers *4*, 1.

Wickersham, M., Wachtel, S., Wong Fok Lung, T., Soong, G., Jacquet, R., Richardson, A., Parker, D., and Prince, A. (2017). Metabolic stress drives keratinocyte defenses against Staphylococcus aureus infection. Cell Rep. *18*, 2742–2751.

Yeung, M., Balma-Mena, A., Shear, N., Simor, A., Pope, E., Walsh, S., and McGavin, M.J. (2011). Identification of major clonal complexes and toxin producing strains among Staphylococcus aureus associated with atopic dermatitis. Microbes Infect. *13*, 189–197.

ISCI, Volume *19*

Supplemental Information

Strains of *Staphylococcus aureus* that Colonize and Infect Skin Harbor Mutations in Metabolic Genes

Karen P. Acker, Tania Wong Fok Lung, Emily West, Joshua Craft, Apurva Narechania, Hannah Smith, Kelsey O'Brien, Ahmed M. Moustafa, Christine Lauren, Paul J. Planet, and Alice Prince

Table S1. Primers used for PCR amplification. Related to Figure 1.

Locus	Primer Sequence (5'-3')	Amplicon size	Source
spa	AACATAGAATTCGCGCAACACGATGAAG CCAATACTCGAGTAGTTCGCGACGACG	**1.3 kb**	**This study**
sea	TTGGAAACGGTTAAAACGAA GAACCTTCCCATCAAAAACA	**120 bp**	**Johnson et al., 1991**
seb	TCGCATCAAACTGACAAACG GCAGGTACTCTATAAGTGCC	**478 bp**	**Johnson et al., 1991**
sek	GGAGAAAAGGCAATGAA TAGTGCCGTTATGTCCA	**516 bp**	**Bania et al., 2016**
Seq	GGAATTACGTTGGCGAA AACTCTCTGCTTGACCA	**330 bp**	**Bania et al., 2016**
sek* and *seq	TAGCATATGCTGATGTAGG AAATATCGACATCCAAATGG	**1.5 kb**	**This study**
IS256	CTAATGGAAAATCAACGAACAG GAATAATCTTTTCTCTTCTGCG	**955 bp**	**This study**
PVL	ATCATTAGGTAAAATGTCTGGACATGATCCA GCATCAASTGTATTGGATAGCAAAAGC	**433 bp**	**This study**
speG	GCCTTATGAATCCTTAACGGAAC TCTGTTTTAAATCCTTGTGACTCG	**498 bp**	**This study**

Table S2. Genome sequence analysis. Related to Figure 1.

Strain	Strain	Coverage on reference	Reference positions touched	de novo contigs >200 nucs	N50	Total assembly size	accession
PE001	6-201	129.5097133	0.955708401	53	148454	2796914	SAMN10689348
PE002	16-660	308.4103519	0.929297595	49	120637	2712274	SAMN10689358
PE003	23-977	226.33487	0.910541732	57	115112	2828524	SAMN10689363
PE004	24-859	190.2588002	0.915070234	416	12627	2695998	SAMN10689365
PE005	31-921	146.1693183	0.939041705	68	103413	2782563	SAMN10689370
PE006	40-808	177.5429384	0.918942955	56	105735	2796571	SAMN10689380
PE007	44-398	206.621994	0.901813315	74	115135	2757172	SAMN10689385
PE008	48-634	390.3148304	0.918614717	71	84800	2880647	SAMN10689389
PE009	43-121	351.3036432	0.956912404	72	86961	2736934	SAMN10689383
PE010	64-515	166.089783	0.916041721	70	77982	2726169	SAMN10689408

Table S3. Primers used for qRT-PCR. Related to Figure 2.

Gene	Primer sequences (5' – 3')
gltA	Forward: GATCTAGCTGAAAACGCGCA Reverse: CTGTCATTGGATGCACGTGA
acnA	Forward: GCAAACATGGCACCAGAGTA Reverse: TTTGGTCCTGAAAGCGATGC
Icd	Forward: CCAGCTGAGCATGATGTTGT Reverse: GGAGCTGTACCATGTGTTGC
sucA	Forward: GCCGTGTTACATGATGAGCA Reverse: CACCATATTGCGCTTCCCAA
sucB	Forward: TGCTATCATCGGCGAAGGTA Reverse: TGACACCATTTTCACGAGCA
sucC	Forward: TAGAGGTAAAGCAGGCGGAG Reverse: CCCTTCTTCAGACGCCATCA
sucD	Forward: GGACCACGTATGCCAGAGAA Reverse: CTGTAAGCCACCAGTACCCA
sdhB	Forward: GGACCACGTATGCCAGAGAA Reverse: CTGTAAGCCACCAGTACCCA
sdhA	Forward: TGTATGGTGGCGACTTCCTT Reverse: TTGTTGTCCAGTTGTTGCCC
fumC	Forward: ATGCTTGACCGTTGCGAAAT Reverse: AGCGCCTTCAATGTTCCATG
menD	Forward: ATCGTTTCAACTGCACTGGG Reverse: AAATACCGCCACCATCGTTG
hemA	Forward: GCCAGGGTTAAGCGAAAGAG Reverse: CTTCGCTTGCTCATGAGGAC
hemB	Forward: TTGCTGAAATTCGTCGTGGA Reverse: TCATCATGTCGCACCCTTCT
16S rRNA	Forward: GCGCTGCATTAGCTAGTTGGT Reverse: GGCCGATCACCCTCTCA

Figure S1.

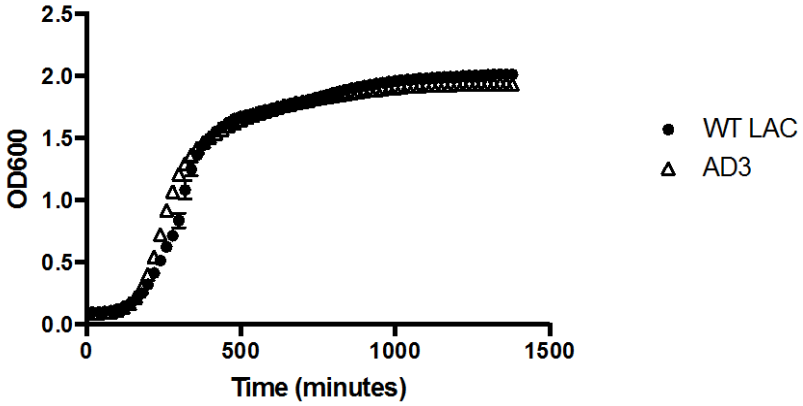

Figure S1. Growth curves of AD3 and WT LAC growth curve grown aerobically in LB. Related to Figure 4 .

Transparent Methods

Contact for Reagent and Resource Sharing

Further information and requests for resources and reagents should be directed to and will be fulfilled by the Lead Contact, Alice Prince (asp7@cumc.columbia.edu).

Experimental Model and Subject Details

Human

Isolates of *S. aureus* were obtained from male and female patients aged 0 to 18 years with AD who presented to Columbia University Medical Center Department of Dermatology. To screen patients for *S. aureus,* a dry, sterile swab (rayon with Amies transport medium, HealthLink) was used to culture from the anterior nares, perianal skin, and one or more skin areas with clinically active AD, clinical evidence of infection, or eroded skin. Swabs were sent to the institution's microbiology lab for routine processing and testing. Severity of AD was quantified by EASI score (Hanifin et al., 2001). Exclusion criteria for screening included age greater than 18 years, inconclusive diagnosis of atopic dermatitis, evidence of acute systemic illness, current use of systemic antibiotics, fungal or viral skin infection, and any individual who declined to participate. Inclusion criteria for microbiological evaluation included laboratory detection of *S. aureus* on culture. All data were collected following approval from Columbia University Institutional Review Board (AAAI5956). Informed consent was obtained from all subjects.

Animal

Male and female mice C57BL/6J mice were purchased from the Jackson Laboratory and were housed under standard conditions at Columbia University Medical Center in New York, NY. All animal experiments were carried out in strict accordance with the recommendations in the Guide for the Care and Use of Laboratory Animals of the NIH, the Animal Welfare Act, and U.S. federal law. The Institutional Animal Care and Use Committee of Columbia University approved the protocol (AAAR5412). None of the mice used in our experiments were previously used for other procedures. Six- to 8-week-old healthy sex-matched mice were inoculated intradermally on the back with $1x10^7$ CFUs *S. aureus* WT LAC or clinical isolates in 100 mL PBS. PBS alone was used as a control. For the memory experiments, mice were initially infected with PBS, WT LAC, or clinical isolate AD3 and re-challenged with WT LAC on day 28 after initial infection. Dermonecrosis areas were measured daily up to 10 days. Punch biopsies (5 mm)

were taken at the site of dermonecrosis and homogenized through 40-mm filters for recovery of *S. aureus*, immune cells by flow cytometry, or supernatant for cytokine analysis.

Cell lines

Human primary keratinocytes (HEKn) were purchased from Gibco and grown in DermaLife K complete medium (Lifeline Cell Technology) supplemented with growth factors (DermaLife K LifeFactors kit, Lifeline Cell Technology), 1% fetal bovine serum (FBS, Gibco) and 1% penicillin/streptomycin (Corning) in a humidified incubator at 37°C with 5% CO2 and were used up to passage 8. HEKn cells were plated 24hrs prior to infection without antibiotics to achieve 3x10^5 cells/ml for Seahorse analysis or 4x10^5 cells/ml for all other experiments.

Bacterial strains

S. aureus strains were grown at 37°C with shaking in Luria-Bertani broth (LB, BD). Bacterial inocula were estimated based on OD_{600} and verified by retrospective plating on LB agar plates to determine colony forming units (CFU). *S. aureus* recovered from mouse skin biopsies were serially diluted and plated on BBL CHROMagar Staph aureus plates and enumerated by counting CFUs.

Method Details

Gene detection

Spa types were obtained by PCR amplification and sequencing of the variable 16S ribosomal rRNA gene region, and assigned according to the Ridom web server (http://www.spaserver.ridom.de). Isolates were assigned a clonal complex using whole genome sequencing (see below). PCR amplification was performed to screen for genes encoding staphylococcus protein A (*spa*), staphylococcal enterotoxin A (*sea*), VB (*seb*), VK (*sek*), VQ (*seq*), presence of both *sek* and *seq*, exotoxin G (*speG*), *IS256*, and Panton-Valentine leucocidin (*PVL*) using an Applied Biosystems Veriti 96-Well Thermal Cycler (Life Technologies). Primer sets are available in Table S1. Genomic DNA was prepared from liquid culture following digestion with 50µM Tris-HCL-10 µM EDTA, 0.3 mg/ml lysostaphin, and 8 units/µL mutanolysin for 1 hour at 37 ºC. DNA was extracted using a DNA Blood and Tissue kit (Qiagen) or Wizard Genomic DNA Purification Kit (Promega). PCR was performed in a 50-µL (for *spa*) or 20-µL (for all other gene targets) reaction mixture at the following amplification for 30 cycles: 30 sec-1 m of denaturation at 95°C, 1

m of annealing at 55°C, 2-4 m of extension at 72°C. All Genomic preparations were outsourced for sequencing of *spa* (Genewiz, Inc.).

Whole genome sequencing

Whole genome sequencing was performed on ten *S. aureus* samples cultured from the skin of patients with high and low EASI scores. DNA was quantified using the Qubit dsDNA High Sensitivity Assay Kit and Qubit Fluorometer (Invitrogen, Life Technologies). Indexed paired-ended libraries were prepared from purified DNA using Nextera XT DNA Sample Preparation Kit according to the manufacturing directions though during PCR clean-up the samples were resuspended in 32.5 µL Resuspending Buffer and only 30 µL of the sample was transferred to the Clean Amplified NTA Plate. The resulting libraries were quantified using the Qubit dsDNA High Sensitivity DNA Kit. Samples were sequenced using pooled paired-end 250 bp runs on the MiSeq Benchtop Sequencer (Illumina Inc.) and data were generated in fastq files for subsequent analysis.

Genome sequence analysis

The paired-end tag reads were assembled *de novo* using ABySS 1.3.2 software and the assembly parameter k=47 (Simpson et al., 2009) (Table S2). Genomes were annotated and compared to known *S. aureus* sequences using the Rapid Annotation using Subsystem Technology (RAST) server (Aziz et al., 2008). Sequences were investigated by employing the protein-specific Basic Local Alignment Search Tool (BLASTP) within GenBank (Altschul et al., 1997) and were considered present if sequence identity was ≥95% with reference gene sequence. Genomes were assigned sequence types (ST) and clonal complexes (CC) by the *S. aureus* MLST typing scheme (available at: https://pubmlst.org/saureus/) (Jolley and Maiden, 2010) using the MLST typing perl script v. 2.16.1 for contigs (available at: https://github.com/tseemann/mlst) (database updated 12/12/2018).

Phylogenetic Analysis

We produced two kinds of phylogenetic matrices for comparison, (*i*) a nucleotide reference-based SNP matrix (NUC-SNP), (*ii*) an amino acid-based, concatenated, orthologous, open-reading-frame matrix (AA-ORF). For the NUC-SNP matrix, SNP calling was performed using SAMtools and MUMmer software on previously sequenced whole gene alignments against the reference genome of USA300 strain TCH1516 (Kurtz et al., 2004; Li et al., 2009). We excluded SNPs that were not biallelic, listed as “heterozygous”, or

had a per base Q score greater than or equal to 20. For preassembled genomes available from public databases, we used whole-genome alignment with reference to the *S. aureus* TCH1516 genome using the show-snps utility of NUCmer (http://mummer.sourceforge.net). Phylogenetic matrices were created by combining results of both SNP calling techniques above. We excluded all regions from the reference genome that have been annotated as mobile genetic elements as previously described (Planet et al., 2015), and we also applied a mask that excluded repetitive sequences from the reference genome that were more than 80% identical at the nucleotide level to another portion of the genome over at least 100 bp in length. For the AA-ORF matrix we determined orthologous gene sets from assembled *S. aureus* isolate genomes using a modified version of the OrthologID pipeline (Chiu et al., 2006) that uses OrthoMCL for gene family clustering (Li et al., 2003).

Maximum likelihood (ML) phylogenies were constructed with the POSIX-threads version of RAxML v8.0.19 (Stamatakis, 2006). For NUC-SNP data we used an ascertainment bias correction and a general time-reversible (GTR) substitution model accounting for among-site rate heterogeneity using the Γ distribution and four rate categories (ASC_GTRGAMMA model) for 100 individual searches with maximum parsimony random-addition starting trees. For the AA-ORF matrix we used the PROT_GAMMA_JTT model and the same search parameters. Node support was evaluated with 1000 nonparametric bootstrap pseudoreplicates filtering the optimal ML tree through the bootstrap trees, so that the shown node support values indicate the percent proportion of bootstrap trees that contained a given internode branch. The genome of MSHR1132, a *Staphylococus argenteus* strain, was used as an outgroup to root the tree. Phylogenetic matrices and tree files are available as supplementary materials (Data S1, Data S2, Data S3, Data S4).

Metabolic gene sequence analysis

The ten proteomes of the clinical isolates were used with the WhatsGNU tool basic function (https://github.com/ahmedmagds/WhatsGNU) where each protein was given a GNU (Gene Novelty Unit) score that was the number of times an exact match was found in the *S. aureus* pan proteome database. GNU scores for key components of the TCA cycle, the glycolytic pathway, and terminal components of the electron transport chain were used to produce a heatmap using pheatmap package in R. The GNU

scores of all the proteins in each isolate were then used to produce a histogram in GraphPad Prism v.7. Proteins less than 50 amino acids were excluded from the histograms.

Infection of human primary keratinocytes

HEKn cells were pretreated with 10ug/ml fibronectin 1 hour prior to infection with or without 0.1M 2-deoxyglucose (2-DG) as indicated. HEKn cells were infected with bacteria at an MOI of 50 and incubated at 37°C with 5% CO2, followed by addition of lysostaphin 10ug/ml at 4 hours and cell detachment with Tryple Express at 24 hours. Supernatants were collected and used for cytotoxicity assays, fumarate measurement, or sent to Eve Technologies (Calgary, Canada) for cytokine analysis. Cytotoxicity was determined by LDH assay using multiply frozen and thawed keratinocytes as a positive control. Fumarate was measured from HEKn supernatant at 5 hours of infection using the Fumarate Assay Kit according to the manufacturer's instructions.

Extracellular flux analysis

Glycolysis was measured by Seahorse technology performed according to the XF Glycolysis Stress Test Kit User Guide. HEKn cells were seeded at 30,000 cells/well in a Seahorse XF24 well plate and incubated at 37°C with 5% CO2. A sensor cartridge was calibrated as per the manufacturers' instructions overnight at 37°C without CO2. On the day of infection, the primary keratinocytes were washed once and media was replaced with XF base medium supplemented with 2 mM glutamine and 10 µg/ml fibronectin 1 hour prior to infection. The cells were infected at an MOI of 50 and incubated at 37°C without CO2 for 3 hours. The oxygen consumption rate (OCR) and extracellular acidification rate (ECAR) were measured using a Seahorse XF24 analyzer. Each measurement cycle consisted of a mixing time of 3 minutes and a data acquisition period of 3 minutes (12 data points). The following reagents were added sequentially at 20-minute intervals: glucose at a final concentration of 10 mM to stimulate glycolysis, oligomycin at 1 µM to suppress oxidative phosphorylation, and 2-DG at 50 mM to inhibit glycolysis. The metabolic activity of the bacteria was determined by adding the same amount of bacteria in XF24 well plates without HEKn cells.

Flow cytometry

Red blood cells were lysed from mouse skin homogenates and immune cells were recovered by centrifugation at 700G at 4°C and washed with FACS buffer (10% FBS and 0.1% sodium azide in PBS).

Cells were stained for 30 min at 4°C in presence of counting beads (Bangs Laboratories) and labeled with a combination of BV605-labelled anti-CD11c, BV421-lalbeled CD86, BV510- labelled CD103, PE-CF594–labelled anti-Ly6C, PerCP-Cy5.5–labelled anti-Ly6G, BV650-labelled anti-NK-1.1, AF700-labelled CD45, APC/Cy7-labeled MHCII, PE-labelled CD207, AF594-labelled anti-CD11b, and Fc block. Analysis of immune cell populations was conducted using BD LSR II (BD Biosciences). Cells in the skin were classified as follows:

Langerhans cells CD45+ CD11b+ CD11c+ MHCII+ CD207+,

Langerhans dendritic cells (DCs) CD45+ CD11b+ CD11c+ MHCII+ CD207+ CD103+,

interstitial macrophages CD45+ Ly6C− CD11b+ CD11c+ MHCII+,

Ly6C- monocytes CD45+ Ly6C− CD11b+ CD11c+ MHCII+,

CD11b+ DCs CD45+ Ly6C+ CD11b+ MHCII+ CD11c+,

neutrophils (PMNs) CD45+ Ly6C+ CD11b+ MHCIILy6G+.

All flow cytometry data were analyzed on FlowJo version 10.

Western blots and Antibodies

HEKn cell lysates were frozen in RIPA (1 mM Tris-HCl, pH7.5, 15 mM NaCl, 0.5 mM 447 EDTA, 0.01% SDS, 0.1% Triton X-100, 0.1% deoxycholate) containing 1x HALT protease inhibitor cocktail (ThermoFisher Scientific). Protein concentrations were quantified using the Precision Red advanced protein kit (Cytoskeleton Inc.) and samples were standardised to a concentration of 100 µg. Blots were run using Bolt mini gels (Invitrogen) and transferred to PVDF membranes (Invitrogen) using the iBlot machine (LifeTechnologies). Antibodies for Hif1α, P-S6, and β-actin were used according to the manufacturer's instructions. Secondary antibodies conjugated to horseradish peroxidase HRP were diluted 1:5000. Images were visualized using a digital chemiluminescent detection imager (ProteinSimple) and ImageJ.

RNA isolation from bacterial cells for qRT-PCR

S. aureus strains were grown overnight and re-inoculated 1:100 in LB at 37°C to an OD_{600} of 1. Bacteria were pelleted, resuspended, and incubated in cell wall lysis mixture (18ug/ml lysostaphin, 8U/ml mutanolysin, 50mg/ml lysozyme in 50uM TRIS-HCl 10uM EDTA pH 7.5) for 30 minutes at 37°C, followed by addition of TRK lysis buffer (Omega Bio-tek). After 10 minutes at room temperature, 70% ethanol was

added and samples were were transferred to E.Z.N.A RNA isolation columns. RNA was isolated following the manufacturer's instructions and treated with DNase using the DNA-free DNA removal kit (Invitrogen). cDNA was synthesized using the high-capacity cDNA reverse transcription kit (Applied Biosystems). Quantitative reverse transcription-PCR (qRT-PCR) was performed using Power SYBR green PCR master mix (Applied Biosystems) in a StepOne Plus thermal cycler (Applied Biosystems). Primers used are listed in Table S3. Data were analyzed using the $\Delta\Delta$CT method.

Quantification and Statistical Analysis

See figure legends for statistical details. Samples without normal distribution were analyzed using the nonparametric Mann-Whitney test. Samples with normal distribution were analyzed with two-tailed Student's t test and one- or two-way ANOVA followed by Dunnet's multiple comparisons test. $p < 0.05$ between groups was considered significant. Outliers were determined by Grubb's test and removed. Statistical analysis was performed using GraphPad Prism Version 7.00 (GraphPad). Data are presented as single points with lines representing mean values or as bar graphs with mean ± SEM.

Data and Software Availability

The sequencing data from this study are available in the NCBI Biosample database under Bioproject number PRJNA520898.

REAGENT or RESOURCE	SOURCE	IDENTIFIER
Antibodies		
Rabbit polyclonal anti-Hif1α	Cayman Chemical	Cat#10006421
Rabbit monoclonal anti-phospho-S6 ribosomal protein	Cell Signaling	Cat#4858
Mouse monoclonal anti-β-actin	Sigma Aldrich	Cat#A5316
BV605-labeled anti-mouse CD11c antibody	Biolegend	Cat#117333; RRID:AB_11204262
BV421-labeled anti-mouse CD86 antibody	Biolegend	Cat#105031; RRID:AB_10898329
BV510-labeled anti-mouse CD103 antibody	Biolegend	Cat#121423; RRID:AB_2562713
PE-CF594–labeled anti-mouse Ly6C antibody	BD Horizon	Cat#562728
PerCP-Cy5.5–labeled anti-mouse Ly6G antibody	Biolegend	Cat#127615; RRID:AB_1877272
BV650-labeled anti-mouse NK-1.1 antibody	Biolegend	Cat#108735; RRID:AB_11147949
AF700-labeled anti-mouse CD45 antibody	Biolegend	Cat#103127; RRID:AB_493714
APC/Cy7-labeled anti-mouse MHCII antibody	Biolegend	Cat#107627; RRID:AB_1659252
PE-labeled anti-mouse CD207 antibody	Biolegend	Cat#144203; RRID:AB_2561498
AF594-labeled anti-mouse CD11b antibody	Biolegend	Cat#101254; RRID:AB_2563231
Anti-mouse CD16/32 antibody	Biolegend	Cat#101319; RRID:AB_1574973
Goat anti-rabbit-HRP	Abcam	Cat#ab205718
Bacterial and Virus Strains		
Staphylococcus aureus USA300 WT LAC	Anthony Richardson, University of Pittsburgh, USA	N/A

Staphylococcus aureus USA300 WT JE2	Michael Otto, National Institute of Allergy and Infectious Diseases USA	N/A
Staphylococcus aureus USA300 WT JE2 *fumC* transposon mutant	Nebraska Transposon Mutant Library	N/A
Staphylococcus aureus AD#1	Isolate from patient	N/A
Staphylococcus aureus AD#2	Isolate from patient	N/A
Staphylococcus aureus AD#3	Isolate from patient	N/A
Staphylococcus aureus AD#4	Isolate from patient	N/A
Staphylococcus aureus AD#5	Isolate from patient	N/A
Staphylococcus aureus AD#6	Isolate from patient	N/A
Staphylococcus aureus AD#7	Isolate from patient	N/A
Staphylococcus aureus AD#8	Isolate from patient	N/A
Staphylococcus aureus AD#9	Isolate from patient	N/A
Staphylococcus aureus AD#10	Isolate from patient	N/A
Chemicals, Peptides, and Recombinant Proteins		
Human fibronectin	Corning	Cat#354008
2-Deoxyglucose	Sigma-Aldrich	Cat#D6134
Lysostaphin	Sigma-Aldrich	Cat#L7386
Power SYBR green PCR master mix	Applied Biosystems	Cat# 4367659
Mutanolysin	Sigma-Aldrich	Cat# M9901
Critical Commercial Assays		
LDH Cytotoxicity Assay	Roche	Cat#11644793001
Fumarate Assay Kit	Abcam	Cat# ab102516
Seahorse XF Glycolysis Stress Test Kit	Agilent	Cat# 103020-100
Qubit dsDNA High Sensitivity Assay Kit	Invitrogen	Cat# Q32851
Nextera XT DNA Library Preparation Kit	Illumina	Cat# FC-131-1024
E.Z.N.A Total RNA Isolation kit	Omega Bio-tek	Cat# R6834-02

Deposited Data		
Experimental Models: Cell Lines		
Human primary keratinocytes, neonatal (HEKn)	Gibco	Cat#C0015C
Experimental Models: Organisms/Strains		
C57BL/6J	Jackson Laboratories	Stock No. 000664
Oligonucleotides		
Primers, see Table S***		
Software and Algorithms		
Seahorse XFe24 analyzer	Agilent	N/A
FlowJo	FlowJo	http://flowjo.com
RAST server		http://rast.theseed.org/FIG/rast.cgi
ABySS 1.3.2		http://www.bcgsc.ca/platform/bioinfo/software/abyss
SAMtools		http://samtools.sourceforge.net/

MUMmer		http://mummer.sourceforge.net/
Prism7	Graphpad	http://www.graphpad.com
Other		